Analysis of Bi-stable Behaviors of FGM Cylindrical Shells

Fukang Liu
Tsinghua University

Abstract

This paper presents a theoretical model to predict the bi-stable property of functionally graded material (FGM) cylindrical shells. The condition that the bi-stability exists is given under the principle of minimum potential energy. There is no bi-stable state in the unstressed shell structure, which is only stable in the initial state. However, the shell with initial stress will have bi-stable configurations when the stress meets certain conditions and the two stable states have two opposite curvatures. The finite element method (FEM) simulation is carried out using the ABAQUS software, and the analysis shows that the numerical results have good correlations with the theoretical prediction.

1 Introduction

Bi-stable structures have a wide application in engineering areas (1; 2; 3; 4). For example, these deployable structures with two stable configurations in a coiled state and an extended state can be applied to space antennas, solar arrays and collapsible booms. Bi-stable cylindrical shells were discovered by Daton-Lovett in 1996 (5). In the earlier studies, Iqbal and Pellegrino *et al.* (6; 7) developed some models to analyze the bi-stable behaviors of the composite structures. Galletly and Guest *et al.* (8; 9) built a beam model and a shell model to predict the bi-stable configurations of the shell. An analytical model with residual stress distribution was proposed by Kebadze *et al.* (10). In 2006, Guest and Pellegrino presented a simple two-parameter model (11). It is assumed that every possible configuration of the shell can be described by an underling cylinder, which has two characteristic parameters. Studies show that isotropic cylindrical shells are not bi-stable and pre-stressed isotropic cylindrical shells have bi-stable configurations (10; 11).

In recent years, some researchers have also carried out several studies about the bi-stable property of the cylindrical shell structures (12; 13; 14; 15). Nie *et al.* studied the effects of piezoelectric layers on the bi-stable behaviors of cylindrical shells (16; 17). The results show that electric fields have obvious influences on the number of stable states of the cylindrical shells. Zhang *et al.* investigated the bi-stable characteristics of anti-symmetric cylindrical shells under the influence of ply angles, moisture and temperature (18; 19; 20; 21).

Functionally Graded Materials (FGMs) are a new types of composites, which were first introduced in the early 1980s by a group of Japanese scientists (22). FGMs are usually composed of ceramic and metallic constituent materials and numerous practical applications in engineering science and modern technology (23; 24; 25; 26; 27; 28). Some studies of the bi-stable behavior of FGM laminated shells have been down (29; 30; 31). This paper investigates the bi-stability of FGM cylindrical shells. The generalized constitutive equations for the FGM cylindrical shells are given, and then, the expression of strain energy for the structural system is formulated. In Section 2.3, the condition for bi-stable behaviors of the shell is derived based on the principle of minimum potential energy. Section 3 presents the experiments. Three FGM cylindrical shell models are considered in the numerical simulation, in which the Young's modulus is incorporated with exponential, linear and power-law variations. The rolled-up radii are compared with the theoretical prediction. Finally Section 4 concludes this article.
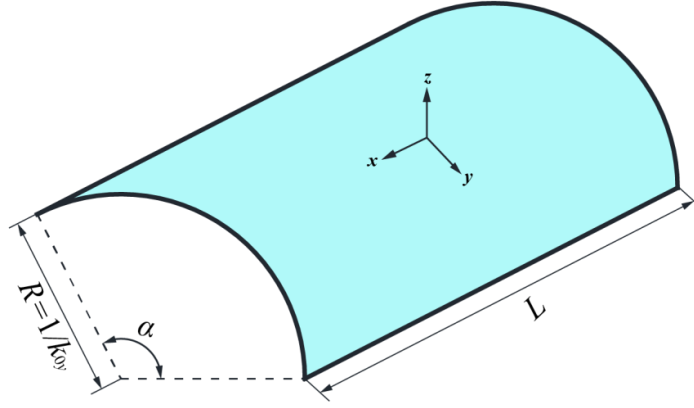
Figure 1: Initial state of the cylindrical shell.

2 Method

2.1 Governing Equations for FGM Cylindrical Shell

The initial configuration of the FGM cylindrical shell is shown in Fig. 1. R represents the initial radius of the shell. k_{0y} is the initial curvature in y-direction. α represents the radius angle and L represents the length of the shell in the longitudinal x-direction. The thickness of the shell is t in z-direction, which is the gradient direction. Material parameters vary along z-direction.

According to the theory of thin shells, the elastic constitutive equations of the cylindrical shell are

$$
\sigma_x = \frac{E(z)}{1 - \mu^2(z)}(\epsilon_x + \mu(z)\epsilon_y)
$$
$$
\sigma_y = \frac{E(z)}{1 - \mu^2(z)}(\epsilon_y + \mu(z)\epsilon_x) \tag{1}
$$
$$
\tau_{xy} = \frac{E(z)}{2(1 + \mu(z))}\gamma_{xy}
$$

where σ_x and σ_y are the normal stresses in the x and y directions, respectively. τ_{xy} is the shear stress in the x-y direction. $E(z)$ and $\mu(z)$ are the Young's modulus and Poisson's ratio along the shell thickness, respectively. The normal strains and shear strain are

$$
\begin{bmatrix} \epsilon_x \\ \epsilon_y \\ \gamma_{xy} \end{bmatrix} = \begin{bmatrix} \epsilon_x^0 \\ \epsilon_y^0 \\ \gamma_{xy}^0 \end{bmatrix} = z \begin{bmatrix} \chi_x \\ \chi_y \\ 2\chi_{xy} \end{bmatrix} \tag{2}
$$

where ϵ_x^0, ϵ_y^0, and γ_{xy}^0 are the mid-plane strains, and χ_x, χ_y, and χ_{xy} are the variance of curvatures, which are expressed by

$$
\chi_x = k_x
$$
$$
\chi_y = k_y - k_{0y} \tag{3}
$$
$$
\chi_{xy} = k_{xy}.
$$

Then the internal force and internal moment in the shell can be expressed as follows

$$
\begin{bmatrix} N_x \\ N_y \\ N_{xy} \\ M_x \\ M_y \\ M_{xy} \end{bmatrix} = \int_{-\frac{t}{2}}^{\frac{t}{2}} \begin{bmatrix} \sigma_x \\ \sigma_y \\ \tau_{xy} \\ z\sigma_x \\ z\sigma_y \\ z\tau_{xy} \end{bmatrix} dz = \begin{bmatrix} A & B \\ B & D \end{bmatrix} \begin{bmatrix} \epsilon_x^0 \\ \epsilon_y^0 \\ \gamma_{xy}^0 \\ \chi_x \\ \chi_y \\ 2\chi_{xy} \end{bmatrix} \tag{4}
$$

2

where

$$\boldsymbol{A} = \begin{bmatrix} K & K_{xy} & 0 \\ K_{xy} & K & 0 \\ 0 & 0 & K_G \end{bmatrix}, \boldsymbol{B} = \begin{bmatrix} P & P_{xy} & 0 \\ P_{xy} & P & 0 \\ 0 & 0 & P_G \end{bmatrix}, \boldsymbol{D} = \begin{bmatrix} D & D_{xy} & 0 \\ D_{xy} & D & 0 \\ 0 & 0 & D_G \end{bmatrix} \quad (5)$$

and

$$K = \int_{-\frac{t}{2}}^{\frac{t}{2}} \frac{E(z)}{1-\mu^2(z)} dz, K_{xy} = \int_{-\frac{t}{2}}^{\frac{t}{2}} \frac{\mu z E(z)}{1-\mu^2(z)} dz, K_G = \int_{-\frac{t}{2}}^{\frac{t}{2}} \frac{E(z)}{2(1+\mu(z))} dz$$

$$P = \int_{-\frac{t}{2}}^{\frac{t}{2}} \frac{E(z)z}{1-\mu^2(z)} dz, P_{xy} = \int_{-\frac{t}{2}}^{\frac{t}{2}} \frac{\mu z E(z)z}{1-\mu^2(z)} dz, P_G = \int_{-\frac{t}{2}}^{\frac{t}{2}} \frac{E(z)z}{2(1+\mu(z))} dz \quad (6)$$

$$D = \int_{-\frac{t}{2}}^{\frac{t}{2}} \frac{E(z)z^2}{1-\mu^2(z)} dz, D_{xy} = \int_{-\frac{t}{2}}^{\frac{t}{2}} \frac{\mu z E(z)z^2}{1-\mu^2(z)} dz, D_G = \int_{-\frac{t}{2}}^{\frac{t}{2}} \frac{E(z)z^2}{2(1+\mu(z))} dz.$$

2.2 Strain Energy Analysis

Iqbal *et al.* (6) proposed a simple model for the bi-stable shell structure. In this model, the longitudinal and transverse curvatures, k_x and k_y, are considered uniform throughout the shell, and no twisting is allowed. It is also assumed that $\boldsymbol{B} = 0$, which means that there is no coupling between stretching and bending. However, in this paper, according to Eqs. (5) and (6), we note that $\boldsymbol{B} \neq 0$, but the coupling behavior has only a weak effect on the bi-stability of the shell (7).

In order to simplify the analysis, it is assumed that $\epsilon_y^0 \approx 0$ and $\gamma_{xy}^0 \approx 0$. The bending energy and the stretching strain energy per unit area have the expressions

$$u_b = \frac{1}{2} \begin{bmatrix} M_x & M_y & M_{xy} \end{bmatrix} \begin{bmatrix} 1 & 0 & 0 \\ 0 & 1 & 0 \\ 0 & 0 & 2 \end{bmatrix} \begin{bmatrix} \chi_x \\ \chi_y \\ \chi_{xy} \end{bmatrix} \quad (7)$$

and

$$u_s = \frac{1}{2} \begin{bmatrix} N_x & N_y & N_{xy} \end{bmatrix} \begin{bmatrix} 1 & 0 & 0 \\ 0 & 1 & 0 \\ 0 & 0 & 2 \end{bmatrix} \begin{bmatrix} \epsilon_x^0 \\ \epsilon_y^0 \\ \gamma_{xy}^0 \end{bmatrix}. \quad (8)$$

Then, substituting Eqs. (3) and (4) into Eqs. (7) and (8) gives

$$u_b = \frac{1}{2}[(P\epsilon_x^0 + D\chi_x + D_{xy}\chi_y)\chi_x + (P_{xy}\epsilon_x^0 + D\chi_y + D_{xy}\chi_x)\chi_y + 4D_G\chi_{xy}^2]$$

$$= \frac{1}{2}[Pk_x + P_{xy}(k_y - k_{0y})]\epsilon_x^0 + \frac{1}{2}[Dk_x^2 + D(k_y - k_{0y})^2 + 2D_{xy}k_x(k_y - k_{0y}) + 4D_Gk_{xy}^2] \quad (9)$$

and

$$u_s = \frac{1}{2}(K\epsilon_x^0 + P\chi_x + P_{xy}\chi_y)\epsilon_x^0 = \frac{1}{2}K(\epsilon_x^0)^2 + \frac{1}{2}(P\chi_x + P_{xy}\chi_y)\epsilon_x^0. \quad (10)$$

The expression of ϵ_x^0 is given by Iqbal *et al.* (6). There, considering

$$\int \epsilon_x^0 ds = \int z k_x ds = \int_{-\frac{\alpha k_y}{2k_{0y}}}^{\frac{\alpha k_y}{2k_{0y}}} \frac{k_x}{k_y}\left[\frac{2k_{0y}\sin(\frac{\alpha k_y}{2k_{0y}})}{\alpha k_y^2} - \frac{\cos\theta}{k_y}\right]d\theta = 0. \quad (11)$$

Then integrating Eqs. (9) and (10) to the whole cross-section of the shell, we can get the bending and stretching strain energies per unit length

$$U_b = \int u_b ds = \frac{\alpha}{2k_{0y}}[Dk_x^2 + D(k_y - k_{0y})^2 + 2D_{xy}k_x(k_y - k_{0y}) + 4D_Gk_{xy}^2] \quad (12)$$

and

$$U_s = \int u_s ds = \frac{K}{2}k_x^2\left[\frac{\alpha}{2k_{0y}k_y^2} + \frac{\sin(\frac{\alpha k_y}{2k_{0y}})}{2k_y^3} - \frac{4k_{0y}\sin^2(\frac{\alpha k_y}{2k_{0y}})}{\alpha k_y^4}\right]. \quad (13)$$
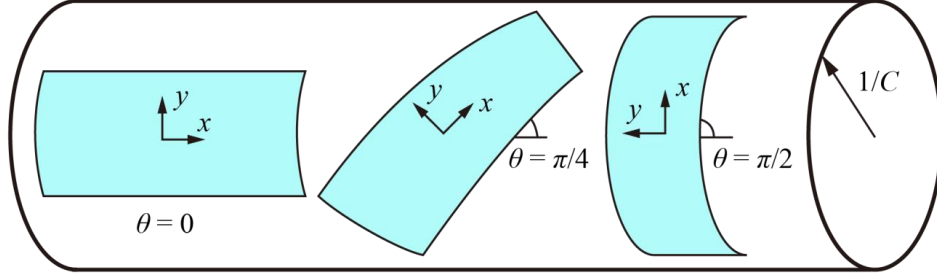
3

Figure 2: Two-parameter model.

In addition, according to Eq. (13), we can obtain

$$\lim_{k_y \to 0} = 0, \text{and } U_s = 0 \text{for } k_y = 0. \tag{14}$$

Thus, the strain energy per unit length for the shell has the expression

$$U = U_b + U_s. \tag{15}$$

2.3 Bi-stability Analysis

Guest and Pellegrino (11) developed a simple two-parameter model for the shell structure. The model neglects the extensional deformation of the mid-surface, and so the Gaussian curvature will be zero. Thus, every possible configuration of the shell can be described by an underling cylinder, which has two characteristic parameters: the curvature of the cylinder, k_c, and the angle of the shell relative to the cylinder, θ, as shown in Fig. 2. The curvatures are expressed by

$$\begin{bmatrix} k_x \\ k_y \\ k_{xy} \end{bmatrix} = \begin{bmatrix} \frac{k_c}{2}(1 - \cos 2\theta) \\ \frac{k_c}{2}(1 + \cos 2\theta) \\ \frac{k_c}{2}\sin 2\theta \end{bmatrix}. \tag{16}$$

In this paper, according to Eq. (14), we can know that when the Gaussian curvature is zero, the stretching strain energy U_s is always zero. Therefore, U_s can be neglected when we analyze the bi-stability of the shell. In addition, from the Eqs. (9), (11) and (12), we can also find that whether or not the mid-surface strains exist does not affect the bending strain energy U_b. As a result, we can use the two-parameter model to simplify the analysis.

Substituting Eq. 16 into Eq. 13 and considering $U_s = 0$, we can get

$$\begin{aligned} U = & \frac{\alpha}{k_{0y}} \Big[D\Big(\frac{1}{4}k_c^2(1 + \cos^2 2\theta) - \frac{1}{2}k_c k_{0y}(1 + \cos 2\theta) + \frac{1}{2}k_{0y}^2\Big) \\ & + D_{xy}\Big(\frac{1}{4}k_c^2(1 + \cos^2 2\theta) - \frac{1}{2}k_c k_{0y}(1 - \cos 2\theta)\Big) \\ & + \frac{1}{2}k_c^2 D_G \sin^2 2\theta \Big]. \end{aligned} \tag{17}$$

Applying the principle of minimum potential energy, we can find the equilibrium position of the shell. Solving the equations $\frac{\partial U}{\partial k_c} = 0$, $\frac{\partial U}{\partial \theta} = 0$ gives two equilibrium configurations

$$\begin{aligned} \theta_1 &= 0 \\ k_{c1} &= k_{0y} \end{aligned} \tag{18}$$

and

$$\begin{aligned} \theta_2 &= \frac{\pi}{2} \\ k_{c2} &= \frac{D_{xy}k_{0y}}{D}. \end{aligned} \tag{19}$$

Furthermore, we need to check whether the two equilibrium configurations are stable equilibria or not. Thus, it is needed to verify if Eqs. (18) and (19 are satisfied Eq. (20).

$$\frac{\partial^2 U}{\partial k_c^2} > 0, \frac{\partial^2 U}{\partial \theta^2} > 0, \text{and } \frac{\partial^2 U}{\partial k_c^2} \frac{\partial^2 U}{\partial \theta^2} - \left(\frac{\partial^2 U}{\partial k_c \partial \theta}\right)^2 > 0 \tag{20}$$

where

$$\frac{\partial^2 U}{\partial k_c^2} = \frac{\alpha}{2k_{0y}} \Big[D(1 + \cos^2 2\theta) + \sin^2 2\theta (D_{xy} + 2D_G) \Big]$$

$$\frac{\partial^2 U}{\partial \theta^2} = \frac{2\alpha}{k_{0y}} k_c \Big[(k_c \cos 4\theta - k_{0y} \cos 2\theta)(D_{xy} - D) + 2k_c D_G \cos 4\theta \Big] \tag{21}$$

$$\frac{\partial^2 U}{\partial k_c \partial \theta} = \frac{\alpha}{k_{0y}} \sin 2\theta \Big[(2k_c \cos 2\theta - k_{0y})(D_{xy} - D) + 4k_c D_G \cos 2\theta \Big].$$

For the first equilibrium position, substituting Eq. (18) into Eq. (21) gives

$$\left(\frac{\partial^2 U}{\partial k_c^2}\right)_1 = \frac{\alpha}{k_{0y}} D > 0,$$

$$\left(\frac{\partial^2 U}{\partial \theta^2}\right)_1 = \frac{4\alpha}{k_{0y}} D_G k_{0y}^2 > 0, \text{and} \tag{22}$$

$$\left(\frac{\partial^2 U}{\partial k_c \partial \theta}\right)_1 = 0.$$

It is obvious that Eq. (22) satisfies Eq. (20), and thus the first equilibrium position is stable. Similarly, for the second equilibrium position, substituting Eq. (19) into Eq. (21) gives

$$\left(\frac{\partial^2 U}{\partial k_c^2}\right)_2 = \frac{\alpha}{k_{0y}} D > 0,$$

$$\left(\frac{\partial^2 U}{\partial \theta^2}\right)_2 = \frac{\alpha}{k_{0y}} \left(\frac{2D_{xy} k_{0y}^2 (D_{xy}^2 + 2D_{xy} D_G - D^2)}{D^2}\right), \text{and} \tag{23}$$

$$\left(\frac{\partial^2 U}{\partial k_c \partial \theta}\right)_2 = 0.$$

According to Eq. (6), we can get

$$\begin{aligned} D_{xy}^2 + 2D_{xy} D_G - D^2 &= D_{xy}(D_{xy} + 2D_G) - D^2 \\ &= D(D_{xy} - D) \\ &= \left(\int_{-\frac{t}{2}}^{\frac{t}{2}} \frac{E(z)z^2}{1 - \mu^2(z)} dz\right) \left(\int_{-\frac{t}{2}}^{\frac{t}{2}} \frac{E(z)(\mu(z) - 1)z^2}{1 - \mu^2(z)} dz\right) < 0. \end{aligned} \tag{24}$$

Then, $\left(\frac{\partial^2 U}{\partial \theta^2}\right)_2 < 0$ in Eq. (23), which means it does not satisfy Eq. (20), and that the second equilibrium position is not stable.

As a result, we can conclude that the unstressed shell with functionally graded material is only stable in the initial state. We consider a mechanical shell model that has the initial stress distribution on the structure. The shell has the bending moment of M_{0x} per unit length with the result of the residue stress. Kebadze *et al.* (10) investigated the bi-stability of a cylindrical shell with a distribution of initial stress. Similarly, in the case of the pre-stressed shell with functionally graded material, the total energy per unit length can be expressed by

$$U = U_1 + U_2 + U_3 \tag{25}$$

where U_1 represents the strain energy in the initial configuration and it is a constant; U_2 and U_3 represents the work done by M_{0x} and the strain energy duo to the change of the curvatures, as shown in Eqs. (26) and (27), respectively.

$$U_2 = \frac{\alpha}{k_{0y}} M_{0x} \chi_x. \tag{26}$$

5

$$U_3 = \frac{\alpha}{2k_{0y}} \left[Dk_x^2 + D(k_y - k_{0y})^2 + 2D_{xy}k_x(k_y - k_{0y}) + 4D_G k_{xy}^2 \right]. \tag{27}$$

Substituting Eqs. (16), (26) and (27) into Eq. (25) gives

$$
\begin{aligned}
U = U_1 + & \left[\frac{k_c}{2}(1 - \cos2\theta)M_{0x} + \frac{1}{2}k_c^2 D_G \sin^2 2\theta \right. \\
& + D\left(\frac{1}{4}k_c^2(1 + \cos^2 2\theta) - \frac{1}{2}k_c k_{0y}(1 + \cos2\theta) + \frac{1}{2}k_{0y}^2 \right) \\
& + \left. D_{xy}\left(\frac{1}{4}k_c^2(1 - \cos^2 2\theta) - \frac{1}{2}k_c k_{0y}(1 - \cos2\theta) \right) \right].
\end{aligned} \tag{28}
$$

Then, solving the equations $\frac{\partial U}{\partial k_c} = 0$ and $\frac{\partial U}{\partial \theta} = 0$, we can get two equilibrium configurations

$$
\begin{aligned}
\theta_1 &= 0 \\
k_{c1} &= k_{0y}
\end{aligned} \tag{29}
$$

and

$$
\begin{aligned}
\theta_2 &= \frac{\pi}{2} \\
k_{c2} &= \frac{D_{xy}k_{0y} - M_{0x}}{D}.
\end{aligned} \tag{30}
$$

It is obvious that Eq. (29) is the same with Eq. (18), and for this equilibrium configuration,

$$
\begin{aligned}
\left(\frac{\partial^2 U}{\partial k_c^2} \right)_1 &= D > 0, \\
\left(\frac{\partial^2 U}{\partial \theta^2} \right)_1 &= 2k_{0y}(M_{0x} + 2D_G k_{0y}), \text{ and} \\
\left(\frac{\partial^2 U}{\partial k_c \partial \theta} \right)_1 &= 0.
\end{aligned} \tag{31}
$$

For the second equilibrium configuration and considering $D_{xy} + 2D_G = D$, we obtain

$$
\begin{aligned}
\left(\frac{\partial^2 U}{\partial k_c^2} \right)_2 &= D > 0, \\
\left(\frac{\partial^2 U}{\partial \theta^2} \right)_2 &= -\frac{(D_{xy}k_{0y} - M_{0x})}{D}(M_{0x} + 2D_G k_{0y}), \text{ and} \\
\left(\frac{\partial^2 U}{\partial k_c \partial \theta} \right)_2 &= 0.
\end{aligned} \tag{32}
$$

When $\left(\frac{\partial^2 U}{\partial \theta^2} \right)_1 > 0$ and $\left(\frac{\partial^2 U}{\partial \theta^2} \right)_2 > 0$ are both satisfied, the first and the second equilibrium positions are stable.

If $M_{0x} \leq 0$, we can get $\left(\frac{\partial^2 U}{\partial \theta^2} \right)_1 \times \left(\frac{\partial^2 U}{\partial \theta^2} \right)_2 \leq 0$, which means they cannot be greater than zero simultaneously. As a result, the shell is not bi-stable.

If $M_{0x} > 0$, when $0 < M_{0x} \leq D_{xy}k_{0y}$, it is clear that $\left(\frac{\partial^2 U}{\partial \theta^2} \right)_1 > 0$ and $\left(\frac{\partial^2 U}{\partial \theta^2} \right)_2 \leq 0$, and then the shell is only stable in the first equilibrium configuration; when $M_{0x} > D_{xy}k_{0y}$, we know that $\left(\frac{\partial^2 U}{\partial \theta^2} \right)_1 > 0$ and $\left(\frac{\partial^2 U}{\partial \theta^2} \right)_2 > 0$. Therefore, the shell is both stable in the two equilibrium positions.

In summarize, when there is an initial bending moment M_{0x} in the shell with functionally graded material, the condition that it has the prosperity of bi-stability is

$$M_{0x} > D_{xy}k_{0y}. \tag{33}$$

In addition, the magnitude of the two rolled-up radii is expressed by

$$R_1 = \frac{1}{k_{0y}}$$
$$R_2 = \frac{D}{M_{0x} - D_{xy}k_{0y}}.$$

(34)

3 Experiments

To verify the theoretical prediction, based on the finite element method with the commercial software ABAQUS, the numerical simulation is conducted to analyze the bi-stable behavior of the FGM cylindrical shell. FGMs are typically made from a mixture of two or more materials. The material properties of FGMs are related to that of the constituent materials. We consider three FGMs models (32; 33; 34; 35). The material properties vary continuously through the thickness direction of the shell. The Young's modulus is incorporated with the exponential, linear and power-law variations, and the Poisson's ratio is assumed to be a constant.

Exponential material variation:

$$E(z) = E_1 \exp\left[m\left(z + \frac{t}{2}\right)\right]$$
$$\mu(z) = \text{constant}$$

(35)

linear material variation:

$$E(z) = E_1 + n\left(z + \frac{t}{2}\right)$$
$$\mu(z) = \text{constant}$$

(36)

and power-law variation:

$$E(z) = E_1 + (E_2 - E_1)\left(\frac{z}{t} + \frac{t}{2}\right)^k$$
$$\mu(z) = \text{constant}$$

(37)

where E_1 and E_2 are the Young's modulus when $z = -\frac{t}{2}$ and $\frac{t}{2}$, respectively. From Eqs. (36) and (37), we can get m and n, which are given in Eq. (38), and k represents the gradient index.

$$m = \frac{1}{t}\ln\left(\frac{E(\frac{t}{2})}{E(-\frac{t}{2})}\right) = \frac{1}{t}\ln\left(\frac{E_2}{E_1}\right)$$
$$n = \frac{E(\frac{t}{2}) - E(-\frac{t}{2})}{t} = \frac{E_2 - E_1}{t}.$$

(38)

The FGMs cylindrical shell is used for our study and its properties are (33): $E_1 = 105.70$ GPa, $E_2 = 168.06$ GPa, and $\mu = 0.3$. When the thickness t is given, we can get m and n. In this paper, $k = 2$.

In order to simplify our analysis, the shell is divided into 20 layers along the z-direction, and the thickness of each layer is $\frac{t}{20}$, as shown in Fig. 3. In each layer, the material properties are homogeneous and isotropic and we set the value of the Young's modulus in the middle surface as the Young's modulus of the whole layer. The Young's modulus of each layer is shown in Eq. (39).

$$E_i = \begin{cases} E_1 \exp\left[\frac{2i-1}{40}\ln\left(\frac{E_2}{E_1}\right)\right], & \text{exponential} \\ E_1 + \frac{2i-1}{40}(E_2 - E_1), & \text{linear} \qquad i = 1, 2, \ldots, 20. \\ E_1 + (E_2 - E_1)\left(\frac{2i-1}{40}\right)^k, & \text{power-law} \end{cases}$$

(39)

In computation, the center point at the shell is restrained in all six degrees of freedom. The edge moment M_{0y} is imposed along the two edges of the longitudinal direction (x-direction) to flatten the shell and it will be removed on the second load step (7), and the initial moment M_{0x} is exerted on the two edges of the y-direction, as mentioned in Section 2.3. The existence of the bi-stable state of the
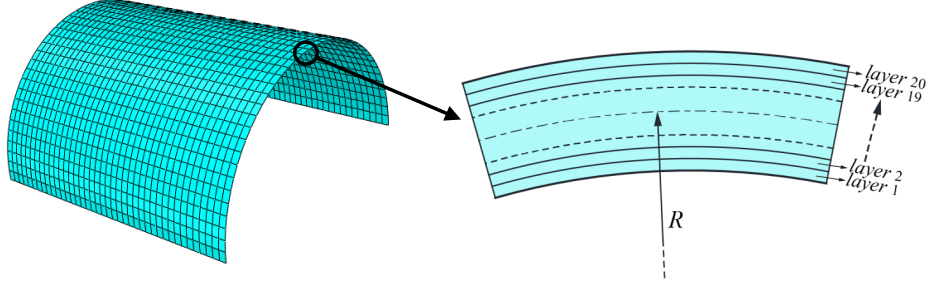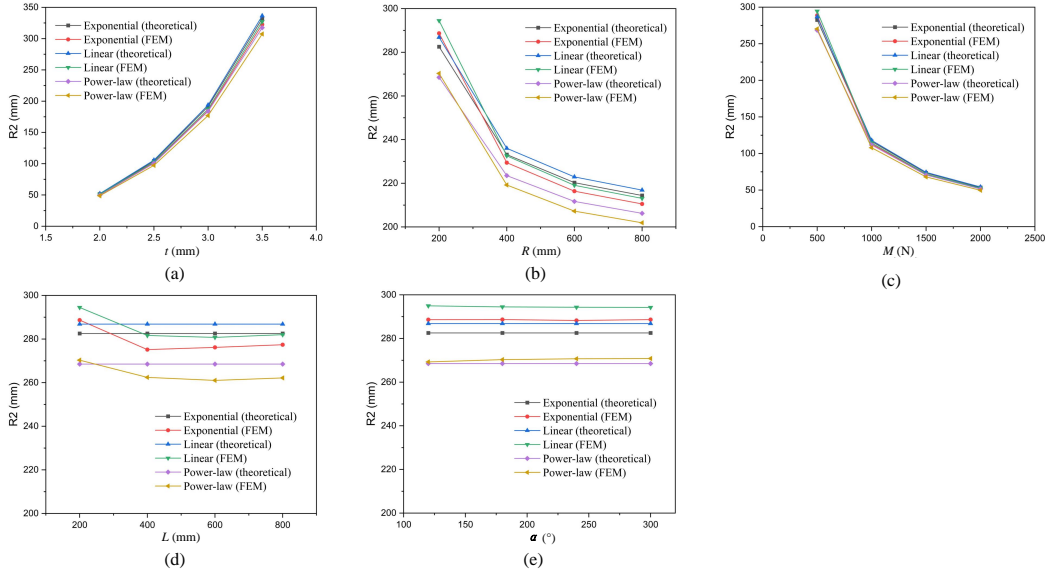
Figure 3: Model of the FGM cylindrical shell.

Figure 4: Effect of the (a) thickness t, (b) initial radius R, (c) initial bending moment M, (d) length L and (e) initial radius angle α on the rolled up radii R_2 of the shell.

shell can be evaluated by Eq. (33). The magnitude of the two rolled-up radii can be calculated by Eq. (34).

Specific examples are carried out and the results are given in Fig. 4 and Tables 1, 2, 3, 4, 5, which respectively show the effect of the thickness, initial radius, bending moment M_{0x}, length and arc central angle on the rolled up radius at the second stable states. In table 4, for the case of $t = 2$mm, $R = 200$mm, $M_{0x} = 500$N, $\alpha = 180°$ and $L = 800$mm, the process of rolling-up the shell is shown in Fig. 5. Fig. 5(a) represents the first stable state, which corresponds to the initial position of the shell. Fig. 5(b) corresponds to the flattened configuration under the action of the edge bending moment M_{0y}. And then, the shell will gradually roll up around the x-direction, as shown in Fig. 5(c). Finally, the second stable position will be reached presented in Fig. 5(d). The unit of stress is MPa.

The theoretical prediction in Eq. (30) is confirmed by the results of the numerical simulation. It can be found that with the increase of the thickness t, the second rolled-up radius will become greater shown in Table 1. With the increase of initial radius R (or $\frac{1}{k_{0y}}$) and moment M_{0x}, the second rolled-up radius will become smaller shown in Tables 2 and 3. In addition, the length L and arc central angle α have no influence on the rolled up radius at the second stable states, as shown in Tables 4 and 5. We can know the numerical results agree well with the theoretical prediction.
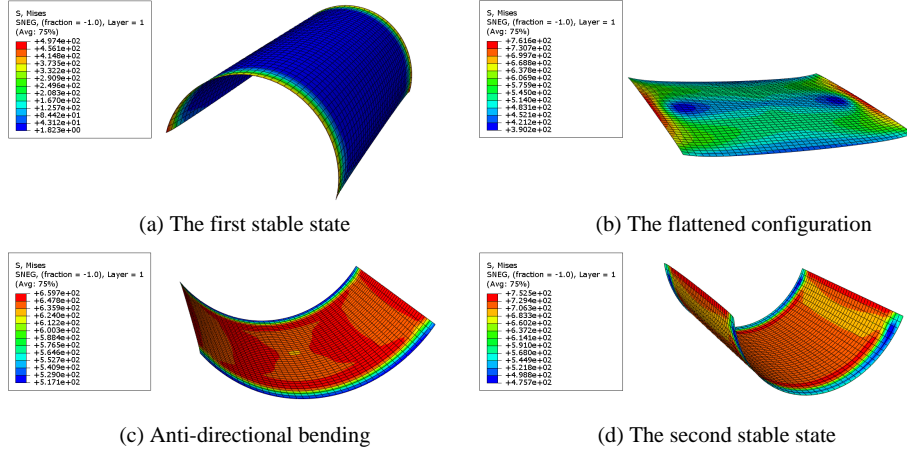
8

(a) The first stable state

(b) The flattened configuration

(c) Anti-directional bending

(d) The second stable state

Figure 5: Finite element deformation.

Table 1: Effect of the thickness on the rolled up radii R_2 of the shell. $R = \frac{1}{k_{0y}} = 400$mm, $M_{0x} = 2000$N, $L = 400$mm, and $\alpha = 180°$

t(mm)	Exponential (mm)		Exponential (mm)		Power-law (mm)	
	theoretical	FEM	theoretical	FEM	theoretical	FEM
2.00	51.53	50.61	52.10	51.21	49.64	48.74
2.50	104.49	101.54	105.69	102.70	100.51	97.37
3.00	191.48	184.99	193.82	187.47	183.77	177.03
3.50	332.11	322.70	336.54	327.21	317.56	307.41

Table 2: Effect of the initial radius on the rolled up radii R_2 of the shell. $t = 2$mm, $M_{0x} = 500$N, $L = 200$mm, and $\alpha = 180°$

R(mm)	Exponential (mm)		Exponential (mm)		Power-law (mm)	
	theoretical	FEM	theoretical	FEM	theoretical	FEM
200	282.55	288.69	286.85	294.49	268.52	270.32
400	233.14	229.42	236.01	232.57	223.51	219.21
600	220.30	216.37	222.91	219.06	211.68	207.25
800	214.40	210.52	216.87	213.07	206.22	201.89

Table 3: Effect of the initial bending moment on the rolled up radii R_2 of the shell. $t = 2$mm, $R = \frac{1}{k_{0y}} = 200$mm, $L = 200$mm, and $\alpha = 180°$

M_{0x}(N)	Exponential (mm)		Exponential (mm)		Power-law (mm)	
	theoretical	FEM	theoretical	FEM	theoretical	FEM
500	282.55	288.69	286.85	294.49	268.52	270.32
1000	116.57	112.93	118.03	114.41	111.75	107.92
1500	73.43	71.00	74.30	71.87	70.56	68.03
2000	53.60	51.84	54.22	52.47	51.56	49.74

Table 4: Effect of the length on the rolled up radii R_2 of the shell. $t = 2$mm, $R = \frac{1}{k_{0y}} = 200$mm, $M_{0x} = 500$N, and $\alpha = 180°$

L(mm)	Exponential (mm)		Exponential (mm)		Power-law (mm)	
	theoretical	FEM	theoretical	FEM	theoretical	FEM
200	282.55	288.69	286.85	294.49	268.52	270.32
400	282.55	275.15	286.85	281.64	268.52	262.42
600	282.55	276.17	286.85	280.76	268.52	261.03
800	282.55	277.39	286.85	282.01	268.52	262.18

Table 5: Effect of the initial radius angle on the rolled up radii R_2 of the shell. $t = 2$mm, $R = \frac{1}{k_{0y}} = 200$mm, $M_{0x} = 500$N, and $L = 200$mm

$\alpha(\circ)$	Exponential (mm)		Exponential (mm)		Power-law (mm)	
	theoretical	FEM	theoretical	FEM	theoretical	FEM
120	282.55	288.63	286.85	294.95	268.52	269.26
180	282.55	288.69	286.85	294.49	268.52	270.32
240	282.55	288.26	286.85	294.30	268.52	270.72
300	282.55	288.66	286.85	294.22	268.52	270.84

4 Conclusion

This paper establishes the theoretical solution of the condition for bi-stability of FGM cylindrical shells based on the principle of minimum potential energy. For the FGM cylindrical shell without pre-stress, the first equilibrium position is stable while the second one is unstable. However, when subjected to initial stress, the shell has bi-stability property if the pre-stress satisfies certain conditions, and the first stable configuration corresponds to the initial state of the shell, while the second stable state has opposite curvature compared to the first condition. Numerical examples are carried out to verify the theoretical model, and it shows that the rolled-up radius of the theoretical prediction agrees well with the numerical simulation.

References

[1] A. S. Panesar and P. M. Weaver, "Optimisation of blended bistable laminates for a morphing flap," *Composite Structures*, vol. 94, no. 10, pp. 3092–3105, 2012.

[2] Y. Xie, Y. Meng, W. Wang, E. Zhang, J. Leng, and Q. Pei, "Bistable and reconfigurable photonic crystals—electroactive shape memory polymer nanocomposite for ink-free rewritable paper," *Advanced Functional Materials*, vol. 28, no. 34, p. 1802430, 2018.

[3] C. Gantes, "An improved analytical model for the prediction of the nonlinear behavior of flat and curved deployable space frames," *Journal of Constructional Steel Research*, vol. 44, no. 1-2, pp. 129–158, 1997.

[4] D. Barbera and S. Laurenzi, "Nonlinear buckling and folding analysis of a storable tubular ultrathin boom for nanosatellites," *Composite Structures*, vol. 132, pp. 226–238, 2015.

[5] A. Daton-Lovett, "An extendible member," *Patent Cooperation Treaty application PCT/GB97/00839*, 1996.

[6] K. Iqbal, S. Pellegrino, and A. Daton-Lovett, "Bi-stable composite slit tubes," in *IUTAM-IASS Symposium on deployable structures: Theory and Applications*. Springer, 2000, pp. 153–162.

[7] K. Iqbal and S. Pellegrino, "Bi-stable composite shells," in *41st Structures, Structural Dynamics, and Materials Conference and Exhibit*, 2000, p. 1385.

[8] D. A. Galletly and S. D. Guest, "Bistable composite slit tubes. i. a beam model," *International Journal of Solids and Structures*, vol. 41, no. 16-17, pp. 4517–4533, 2004.

[9] ——, "Bistable composite slit tubes. ii. a shell model," *International Journal of Solids and Structures*, vol. 41, no. 16-17, pp. 4503–4516, 2004.

[10] E. Kebadze, S. Guest, and S. Pellegrino, "Bistable prestressed shell structures," *International Journal of Solids and Structures*, vol. 41, no. 11-12, pp. 2801–2820, 2004.

[11] S. Guest and S. Pellegrino, "Analytical models for bistable cylindrical shells," *Proceedings of the Royal Society A: Mathematical, Physical and Engineering Sciences*, vol. 462, no. 2067, pp. 839–854, 2006.

[12] X. Jiang, M. Pezzulla, H. Shao, T. K. Ghosh, and D. P. Holmes, "Snapping of bistable, pre-stressed cylindrical shells," *EPL (Europhysics Letters)*, vol. 122, no. 6, p. 64003, 2018.

[13] Y. Wang, L. Peng, and Z. Huang, "Structural optimum design of bistable cylindrical shell for broadband energy harvesting application," *Theoretical and Applied Mechanics Letters*, vol. 5, no. 4, pp. 151–154, 2015.

[14] B. Wang and K. S. Fancey, "A bistable morphing composite using viscoelastically generated prestress," *Materials Letters*, vol. 158, pp. 108–110, 2015.

[15] P. Pavliuchenko, M. Teller, M. Grüber, and G. Hirt, "A semianalytical model for the determination of bistability and curvature of metallic cylindrical shells," *Journal of Manufacturing and Materials Processing*, vol. 3, no. 1, p. 22, 2019.

[16] B. Wang and G. H. Nie, "Analysis of bi-stable behavior of isotropic cylindrical shell structures attached by piezoelectric layers," *Chinese Quarterly of Mechanics*, vol. 35, no. 1, pp. 10–21, 2014.

[17] B. Wang and G.-H. Nie, "Bi-stable states of initially stressed elastic cylindrical shell structures with two piezoelectric surface layers," *Acta Mechanica Sinica*, vol. 31, no. 5, pp. 653–659, 2015.

[18] Z. Zhang, H. Wu, H. Wu, X. He, Y. Bao, and G. Chai, "Bistable characteristics of irregular anti-symmetric lay-up composite cylindrical shells," *International Journal of Structural Stability and Dynamics*, vol. 13, no. 06, p. 1350029, 2013.

[19] Z. Zhang, H. Wu, G. Ye, J. Yang, S. Kitipornchai, and G. Chai, "Experimental study on bistable behaviour of anti-symmetric laminated cylindrical shells in thermal environments," *Composite Structures*, vol. 144, pp. 24–32, 2016.

[20] Z. Zhang, G. Ye, H. Wu, J. Yang, S. Kitipornchai, and G. Chai, "Bistable behaviour and microstructure characterization of carbon fiber/epoxy resin anti-symmetric laminated cylindrical shell after thermal exposure," *Composites Science and Technology*, vol. 138, pp. 91–97, 2017.

[21] Z. Zhang, H. Pan, H. Wu, S. Jiang, and G. Chai, "Hygroscopic influence on bistable characteristics of antisymmetric composite cylindrical shells: An experimental study," *Journal of Composite Materials*, vol. 52, no. 26, pp. 3565–3577, 2018.

[22] M. Koizumi, "Fgm activities in japan," *Composites Part B: Engineering*, vol. 28, no. 1-2, pp. 1–4, 1997.

[23] V. Birman and L. W. Byrd, "Modeling and analysis of functionally graded materials and structures," 2007.

[24] A. Gupta and M. Talha, "Recent development in modeling and analysis of functionally graded materials and structures," *Progress in Aerospace Sciences*, vol. 79, pp. 1–14, 2015.

[25] M. Mahinzare, H. Ranjbarpur, and M. Ghadiri, "Free vibration analysis of a rotary smart two directional functionally graded piezoelectric material in axial symmetry circular nanoplate," *Mechanical Systems and Signal Processing*, vol. 100, pp. 188–207, 2018.

[26] Y. Tlidji, A. R. K. EL-DALABEEH, N. H. AL-OLIMAT, and M. O. AL SHBAIL, "Vibration analysis of different material distributions of functionally graded microbeam," *Structural Engineering and Mechanics, An Int'l Journal*, vol. 69, no. 6, pp. 637–649, 2019.

[27] N. D. Duc, K. Seung-Eock, and D. Q. Chan, "Thermal buckling analysis of fgm sandwich truncated conical shells reinforced by fgm stiffeners resting on elastic foundations using fsdt," *Journal of Thermal Stresses*, vol. 41, no. 3, pp. 331–365, 2018.

[28] A. Fallah and M. Aghdam, "Thermo-mechanical buckling and nonlinear free vibration analysis of functionally graded beams on nonlinear elastic foundation," *Composites Part B: Engineering*, vol. 43, no. 3, pp. 1523–1530, 2012.

[29] X. He, L. LI, S. KITIPORNCHAI, C. Wang, and H. Zhu, "Bi-stable analyses of laminated fgm shells," *International Journal of Structural Stability and Dynamics*, vol. 12, no. 02, pp. 311–335, 2012.

[30] L. Li, X. He, H. Zhu, and S. Kitipornchai, "Bistable characteristic of laminated shells with graded fibers," *International Journal of Mechanics and Materials in Design*, vol. 7, no. 3, pp. 219–229, 2011.

[31] Z. Zhang, Y. Bao, and H. Sun, "Research on the bistablity of fgm laminate plates," in *2010 International Conference on Electrical and Control Engineering*. IEEE, 2010, pp. 2960–2963.

[32] J.-H. Kim and G. Paulino, "Isoparametric graded finite elements for nonhomogeneous isotropic and orthotropic materials," *J. Appl. Mech.*, vol. 69, no. 4, pp. 502–514, 2002.

[33] D. Van Dung *et al.*, "Nonlinear torsional buckling and postbuckling of eccentrically stiffened fgm cylindrical shells in thermal environment," *Composites Part B: Engineering*, vol. 69, pp. 378–388, 2015.

[34] H. Huang and Q. Han, "Nonlinear buckling of torsion-loaded functionally graded cylindrical shells in thermal environment," *European Journal of Mechanics-A/Solids*, vol. 29, no. 1, pp. 42–48, 2010.

[35] K. Daneshjou, M. Shokrieh, M. G. Moghaddam, and R. Talebitooti, "Analytical model of sound transmission through relatively thick fgm cylindrical shells considering third order shear deformation theory," *Composite Structures*, vol. 93, no. 1, pp. 67–78, 2010.